RESEARCH ARTICLE

AMERICAN JOURNAL OF BOTANY

Cell autonomous sanctions in legumes target ineffective rhizobia in nodules with mixed infections[1]

John U. Regus[2], Kenjiro W. Quides[2], Matthew R. O'Neill[2], Rina Suzuki[2], Elizabeth A. Savory[3], Jeff H. Chang[3], and Joel L. Sachs[2,4-6]

PREMISE OF THE STUDY: To maximize benefits from symbiosis, legumes must limit physiological inputs into ineffective rhizobia that nodulate hosts without fixing nitrogen. The capacity of legumes to decrease the relative fitness of ineffective rhizobia—known as sanctions—has been demonstrated in several legume species, but its mechanisms remain unclear. Sanctions are predicted to work at the whole-nodule level. However, whole-nodule sanctions would make the host vulnerable to mixed-nodule infections, which have been demonstrated in the laboratory and observed in natural settings. Here, we present and test a cell-autonomous model of legume sanctions that can resolve this dilemma.

METHODS: We analyzed histological and ultrastructural evidence of sanctions in two legume species, *Acmispon strigosus* and *Lotus japonicus*. For the former, we inoculated seedlings with rhizobia that naturally vary in their abilities to fix nitrogen. In the latter, we inoculated seedlings with near-isogenic strains that differ only in the ability to fix nitrogen.

KEY RESULTS: In both hosts, plants inoculated with ineffective rhizobia exhibited evidence for a cell autonomous and accelerated program of senescence within nodules. In plants that received mixed inoculations, only the plant cells harboring ineffective rhizobia exhibited features consistent with programmed cell death, including collapsed vacuoles, ruptured symbiosomes, and bacteroids that are released into the cytosol. These features were consistently linked with ultrastructural evidence of reduced survival of ineffective rhizobia *in planta*.

CONCLUSIONS: Our data suggest an elegant cell autonomous mechanism by which legumes can detect and defend against ineffective rhizobia even when nodules harbor a mix of effective and ineffective rhizobial genotypes.

KEY WORDS *Bradyrhizobium*; coinfection; Fabaceae; host control; induced nodule senescence; legume rhizobium mutualism; *Mesorhizobium*; nitrogen fixation; programmed cell death; symbiont cheating

Diverse species of legumes form symbiotic root nodules in which rhizobia fix nitrogen for the plant hosts in exchange for photosynthates (Soltis et al., 1995). However, rhizobial genotypes vary substantially in the amount of nitrogen they fix for legume hosts and often include ineffective genotypes that instigate nodule formation but fail to fix any nitrogen (Quigley et al., 1997; Burdon et al., 1999; Denton et al., 2000; Collins et al., 2002; Simms et al., 2006; Heath and Tiffin, 2009; Sachs et al., 2010a). Fixing nitrogen requires rhizobia to expend enormous amounts of energy; therefore, rhizobia that bypass this step can gain advantage by accessing plant resources without paying the costs of nitrogen fixation (Porter and Simms, 2014; Ratcliff and Denison, 2008; Sachs et al., 2010a; Trainer and Charles, 2006; West et al., 2002a). To maximize fitness benefits from symbiosis, legumes must limit their physiological inputs into supporting ineffective rhizobia (Denison, 2000; Sachs et al., 2004).

The legume–rhizobium symbiosis is initiated when the host plant releases flavonoids into the soil that attract rhizobia, and in response, the rhizobia secrete nod factors that trigger morphological changes in the plant. Upon entering root cortical cells, the bacteria are encased by a plant-derived membrane and live in organelle-like structures called symbiosomes in which they differentiate into bacteroids and can fix nitrogen (Jones et al., 2007). Legume nodules superficially resemble lateral roots, but harbor the bacteroids in a

[1] Manuscript received 5 May 2017; revision accepted 11 August 2017.

[2] Department of Evolution, Ecology, and Organismal Biology, 2710 Life Sciences Building, University of California, Riverside, California 92521 USA;
[3] Department of Botany and Plant Pathology, Cordley Hall, 2701 SW Campus Way, Oregon State University, Corvallis, Oregon 97331 USA;
[4] Department of Botany and Plant Sciences, 2142 Batchelor Hall, University of California, Riverside, California 92521 USA; and
[5] Institute for Integrative Genome Biology, 5406 Boyce Hall, University of California, Riverside, California 92521 USA
[6] Author for correspondence (e-mail: joels@ucr.edu), phone: (951) 827-6357; ORCID id 0000-0002-0221-9247

https://doi.org/10.3732/ajb.1700165

central region of the nodule in which infected and interstitial cells (that do not harbor bacteroids) are interspersed and are surrounded by the nodule cortex, which remains uninfected. Nodule development varies among legume taxa. Determinate nodules, such as those in *Lotus japonicus* and *Acmispon strigosus* studied here, lack a continuous meristem, have bacteroids at similar stages of differentiation, cease growth after their development is complete, and allow nitrogen-fixing rhizobia to escape back into the soil during nodule senescence (the bacteroids do not terminally differentiate; Mergaert et al., 2006). In contrast, indeterminate nodules, such as those in *Medicago truncatula*, grow throughout the functional association, with a spatial gradation of bacteroids in different developmental stages. In *Medicago*, the bacteroids terminally differentiate and cannot escape the nodule (Mergaert et al., 2006), but nonetheless, a subset of undifferentiated rhizobia can be released upon nodule senescence (Paau et al., 1980).

Previous work suggested that before nodule formation, legumes have little capacity to assess rhizobial symbionts for their potential to fix nitrogen. While some legumes can distinguish between genetically diverged rhizobia that vary in symbiotic effectiveness or toxicity (Devine et al., 1990; Devine and Kuykendall, 1996; Heath and Tiffin, 2009; Sachs et al., 2010b), host plants that are coinoculated with effective rhizobia and near-isogenic strains lacking nitrogen fixation function are often nodulated with equal frequency by both (Amarger, 1981; Hahn and Studer, 1986). After nodule development is underway, several legume species show the capacity to selectively punish ineffective rhizobia. Experiments have demonstrated that nodules with nitrogen-fixing rhizobia typically grow (and the rhizobia within them proliferate rapidly), whereas nodules with ineffective or less-effective rhizobia tend to stay small (and the rhizobia within them have reduced fitness) (Kiers et al., 2003; Simms et al., 2006; Sachs et al., 2010b; Oono et al., 2011; Regus et al., 2014, 2015). This capacity of legume hosts to target ineffective and less-effective rhizobia and reduce their fitness relative to beneficial genotypes is termed "sanctions" (Kiers et al., 2003; Sachs et al., 2010b; Oono et al., 2011). Evidence exists for sanctions in legumes with both determinate and indeterminate nodules, but there are also exceptions (Marco et al., 2009; Gubry-Rangin et al., 2010). Beyond this general phenotypic pattern, however, there is little understanding of the mechanistic bases of legume sanctions in either type of nodule.

The dominant models of legume sanctions include the prediction that legumes sense and respond to symbiotic benefit from individual nodules (Denison, 2000; West et al., 2002a, b; Friesen and Mathias, 2010). Under the 'whole-nodule' model of sanctions, nodules infected by multiple genotypes (mixed infections) would allow ineffective rhizobia to proliferate without detection, thus decreasing the efficiency of sanctions and promoting the fitness of ineffective genotypes (West et al., 2002a, b; Friesen and Mathias, 2010). However, in studies of field-grown host plants, multiple rhizobial genotypes have been found within individual nodules (Moawad and Schmidt, 1987; Simms et al., 2006; van Berkum et al., 2012) and these observations have been recapitulated in the laboratory on multiple legume species (Johnston and Beringer, 1975; Labandera and Vincent, 1975; Brockwell et al., 1977; Bromfield and Jones, 1980; Amarger, 1981; Hahn and Studer, 1986; Gage, 2002; Simms et al., 2006; Heath and Tiffin, 2009; Sachs et al., 2010b; Checcucci et al., 2016). Moreover, work has shown that legumes with determinate nodules can efficiently sanction ineffective rhizobia even when the majority of the nodules are coinfected with a mixture of effective and ineffective rhizobial genotypes (Sachs et al., 2010b; Regus et al., 2014). The whole-nodule model of sanctions does not adequately account for sanctioning in nodules infected with mixtures of effective and ineffective genotypes.

For legumes with determinate nodules, a potential mechanism for legume sanctions derives from histological observations that nodules with ineffective rhizobia undergo an accelerated schedule of nodule senescence (Chua et al., 1985; Banba et al., 2001; Schumpp and Deakin, 2010; Chungopast et al., 2014). Nodule senescence is a natural process by which the nodule organ breaks down (Thomas, 2013), and two potential triggers have been described. Developmental nodule senescence often occurs when the host is setting fruit, when plants must shift carbon resources toward seed production rather than support nitrogen fixation in the nodule. In this case, nodule senescence is part of nodule maturation and is likely critical for release of the symbionts into the soil (Denison and Kiers, 2004; Puppo et al., 2005). In contrast, induced nodule senescence only occurs when host plants experience stress, such as prolonged darkness (Gogorcena et al., 1997), water deficiency (González et al., 1998), and failure of the plant to recognize the bacteria (Banba et al., 2001). The morphological changes associated with induced nodule senescence are distinguishable from those of developmental nodule senescence. In induced nodule senescence, changes progress faster, and the contents of the symbiosome can be degraded without cellular evidence for vesicle trafficking that might indicate nutrient remobilization (Pérez Guerra et al., 2010). Histological evidence suggests that induction of nodule senescence can be cell autonomous (Maunoury et al., 2010). Moreover, induced senescence shares key features of programmed cell death in plants. Programmed cell death is initiated when the tonoplast surrounding the vacuole ruptures, which releases enzymes that degrade the cytoplasmic contents, nuclei, and organelles (van Doorn, 2011), similar to what has been observed in nodules with ineffective rhizobia (Chua et al., 1985; Banba et al., 2001; Schumpp and Deakin, 2010; Chungopast et al., 2014).

Here we test a cell-autonomous model of legume sanctions in species with determinate nodules. Our model predicts that sanctions occur at the level of individually infected plant cells and thus can generate localized effects within nodules that contain multiple rhizobial genotypes. We investigated this model in *Acmispon strigosus* (formerly *Lotus strigosus*) and *Lotus japonicus*, which are New World and Old World members, respectively, of the *Loteae* tribe (Allan and Porter, 2000; Degtjareva et al., 2006). *Acmispon strigosus* is typically nodulated by *Bradyrhizobium* spp. (Sachs et al., 2009) and has been demonstrated to efficiently sanction ineffective *Bradyrhizobium* (decrease the relative fitness of ineffective strains) even when a significant portion of nodules contain a mixture of effective and ineffective genotypes (Sachs et al., 2010b; Regus et al., 2014). *Lotus japonicus* is nodulated by *Mesorhizobium loti* and the *Lotus–Mesorhizobium* interaction is a model for the development and genomics of symbiosis (Handberg and Stougaard, 1992; Sato et al., 2008). *Acmispon strigosus* hosts were experimentally inoculated with a panel of four characterized native *Bradyrhizobium* genotypes ranging from highly effective to ineffective (Sachs et al., 2009; Sachs et al., 2010a). *Lotus japonicus* hosts were inoculated with the wild-type strain *M. loti* MAFF303099 (expressing DsRed) or with the near-isogenic mutant STM-6 (expressing GFP), which has a transposon inserted in the nitrogenase gene *nifD* and is thus incapable of fixing nitrogen (Shimoda et al., 2008). In clonally infected and coinfected hosts we quantified histological features of programmed cell death, including vacuolar rupture and senescence of infected nodule cells, as well as ultrastructural evidence linked to rhizobial fitness, including rupture of symbiosomes, evidence of bacteroids released into the cytosol, and

estimates of bacteroid population densities within cells. These data were analyzed in singly infected nodules that house different rhizobial genotypes and were compared between singly infected and coinfected nodules in a temporal series.

MATERIALS AND METHODS

Inoculation and dissection protocols—*Acmispon strigosus* seeds were collected from parental plants at Bodega Marine Reserve (BMR; 38.319°N, −123.064°W), where *A. strigosus* host plants were demonstrated to exhibit efficient sanctions against sympatric ineffective *Bradyrhizobium* (Sachs et al., 2010b; Regus et al., 2014). *Lotus japonicus* MG-20 seeds were acquired from LegumeBase (Miyazaki, Japan). MG-20 is an early-flowering genotype that thrives in indoor settings (Kawaguchi, 2000). *Acmispon strigosus* and *L. japonicus* seeds were germinated under sterile conditions and grown in insect-free greenhouses to generate selfed offspring seeds for experiments. Seedlings were prepared for inoculation following published protocols (Sachs et al., 2009).

Bacterial strains—Four previously characterized *Bradyrhizobium* genotypes, referred to as strain number (#) 2, 24, 38, and 49, were used to inoculate *A. strigosus* (Sachs et al., 2009, 2010a). All four *Bradyrhizobium* genotypes were isolated from *A. strigosus* at BMR (Sachs et al., 2009). Genotypes #49, #24, and #38 provide a relative growth benefit to *A. strigosus* of ~500%, ~390%, and ~380%, respectively, based on increase in shoot biomass compared to uninfected controls (Sachs et al., 2010a). Genotype #2 instigates nodule formation on sympatric *A. strigosus*, but does not enhance host growth (i.e., ineffective). For clarity, the *Bradyrhizobium* strains are hereafter referred to based upon their percentage growth benefit percentage to hosts (i.e., strains Br500, Br390, Br380, and Br0). Measures of nitrogen fixation based on $\partial^{15}N$ analysis confirmed that the differences in host growth response among *Bradyrhizobium* genotypes are consistent with their differences in nitrogen fixation (Regus et al., 2014). For *M. loti* genotypes, we used the type strain MAFF303099 (MAFF) expressing DsRed, which is integrated into the genome (Maekawa et al., 2009) and a near-isogenic Fix^- mutant generated by a signature tagged transposon inserted in the *nifD* gene (mlr5906, strain ID 17T02d02, STM-6; Shimoda et al., 2008). A pBBR1-MCS2 plasmid carrying GFP downstream of a constitutive promoter (Chang et al., 2005) was inserted into STM-6. The cells were grown overnight, pelleted, washed with sterile water, and mixed at a ratio of 8:1:1 for recipient, donor, and pRK2013 helper in a total of 20 μL and incubated overnight at 28°C. Cells were selected on 100 μg/mL streptomycin, 100 μg/mL spectinomycin, 100 μg/mL phosphomycin (for the STM mutants), and 50 μg/mL kanamycin (for the GFP plasmid). We found no evidence of loss of DsRed or GFP during plant infection or *in vitro* growth.

Bradyrhizobium and *Mesorhizobium* genotypes were grown on a modified arabinose gluconate medium (MAG; Sachs et al., 2009), and inocula were prepared by picking single-plated colonies of each genotype, adding them individually to liquid MAG, and growing them until saturation (29°C, 180 rpm, 96 h). We quantified doubling time *in vitro* to examine the potential role of growth rate differences on nodulation rate and *in planta* proliferation and to test whether ineffective genotypes are compromised for fitness. *In vitro* growth was quantified in liquid MAG via serial dilution of replicate cultures and plating at multiple time points.

Inoculations—Host plants for inoculation were grown in sterile quartzite sand soil with no source of mineral nitrogen and were fertilized with nitrogen-free Jensen's solution, which provides macro- and micronutrients except for nitrogen (Somasegaran and Hoben, 1994). For singly inoculated plants, seedlings each received 5×10^8 rhizobial cells (in 5 mL, pipetted into the soil). For coinoculations, seedlings each received 5×10^8 rhizobial cells that included either an equal mix of effective and ineffective rhizobial genotypes for *A. strigosus* or a range of ratios for *L. japonicus* (effective to ineffective 3:7, 1:19). An equal ratio was used for *A. strigosus* because it generated high rates of nodule coinfection in previous studies (Sachs et al., 2010b; Regus et al., 2014). A range of ratios was used for *L. japonicus* based upon data from pilot experiments.

Acmispon strigosus plants were grown in greenhouses under ambient conditions from February to June and were harvested at multiple times (3–9 wk postinoculation; wpi). During harvest, plants were carefully removed from pots, and the roots were washed in tap water to remove all traces of soil. *Lotus japonicus* plants for light microscopy and TEM were grown in an environmental growth chamber in sterile plant pouches filled with N-free Jensen's solution and maintained at 20°C with 14 h light/10 h dark. *Lotus japonicus* plants for confocal microscopy were grown in the greenhouse in March and April because previous experiments confirming nodule coinfection were done under these conditions (Sachs et al., 2010b; Regus et al., 2014). For both host species, nodules were dissected by excising 1 mm of root tissue on either side of an intact nodule to determine orientation during sectioning. A minimum of five nodules were sampled from at least two plants per treatment. Harvest time points overlap with the period in which bacteroid differentiation is complete and nitrogen fixation occurs.

Light microscopy—Nodules were fixed in 4% v/v paraformaldehyde, 2.5% v/v glutaraldehyde in 50 mM phosphate buffer pH 7.2 for 3 h at 20°C, then 4°C overnight, and dehydrated in a graded alcohol series to 100% ethanol. Nodules were then infiltrated in JB4 methacrylate (Polysciences, Warrington, Pennsylvania, USA) in a graded series of catalyzed Solution A and 100% ethanol (1:1 and 3:2) with gentle agitation for 8 h on a rotary mixer at room temperature and stored at 4°C overnight. Finally, the samples were infiltrated with catalyzed Solution A (100%) and embedded in film caps in JB4 methacrylate on ice. Specimens were individually removed with a hand saw and repolymerized on metal stubs for sectioning. Sections were prepared parallel to the long axis of the parent root. Sections measuring 4 μm were cut on a Porter-Blum Microtome (ThermoFisher, Pittsburgh, Pennsylvania, USA), mounted on glass slides, and stained with 0.1% w/v aqueous toluidine blue O. Slides were covered in #1.5 coverslips using Permount (ThermoFisher). Images were acquired with a Leica DM 4000B microscope (Wetzlar, Germany) and a Keica DFC 490 digital camera (Utsunomiya, Japan).

Transmission electron microscopy—Nodules were fixed overnight in 2.2% v/v glutaraldehyde, 1.8% v/v paraformaldehyde, 50 mM phosphate buffer, pH 7.2 at 4°C, rinsed three times in 50 mM phosphate buffer (15 min each), and postfixed in 2.5 w/v the OsO_4 and rinsed twice with dH_20, the samples were dehydrated in a graded acetone series to 100% acetone. Nodules were infiltrated in a graded series of Spurr's resin (Spurr's standard mix; EMS, Hatfield, Pennsylvania, USA) on a rotator to 100% Spurr's, embedded in fresh Spurr's resin and polymerized at 70°C overnight. Individual nodules were cut out of blocks of Spurr's resin and re-embedded in

molds for sectioning. Sections of 50 nm thickness were prepared parallel to the long axis of the parent root with an ultramicrotome (Leica RMC XT-X), collected on copper grids and counterstained with lead citrate (0.4%, 10 min) and uranyl acetate (1% w/v, 20 min) at room temperature in a CO_2-free environment. Images were acquired with a Tecnai12 TEM (ThermoFisher) and Gatan US1000 HR CCD Camera (Pleasanton, California, USA).

Confocal microscopy—Nodules were embedded in 6% w/v agarose and sectioned at 70 μm thickness with an Oscillating Tissue Slicer (EMS 5000) parallel to the long axis of the parent root. Sections were imaged with a Leica TCS SP2 laser scanning confocal microscope (Wetzlar) using 488 nm (Argon) and 543 nm (HeNe) excitation beams. Emission ranges of 500–535 nm and 580–600 nm were used to detect GFP and DsRed expression, respectively. To minimize autofluorescence associated with developmental nodule senescence, we did not analyze nodules of plants that were at or beyond the flowering stage.

Data analysis—Histological and ultrastructural data were analyzed using ImageJ software (Schneider et al., 2012). Histological features of nodule senescence were analyzed by following a classic model of plant programmed cell death, where "autophagic" cell death is initiated by vacuolar rupture, followed by destruction of the cytoplasm and eventual senescence of the cell wall (van Doorn, 2011). We first counted and measured the cell areas of three distinct cell types within nodules; infected cells (identified by toluidine blue staining of intracellular bacteroids), interstitial cells (within the infected region, but not harboring bacteroids), and cortex cells (i.e., the uninfected nodule cortex made up of vascular bundles and parenchymatous cells that transport fixed nitrogen from bacteroids to the tissues of the plant (Pérez Guerra et al., 2010)). For each of these cell types, we quantified cells undergoing senescence, defined as cells with a blotchy appearance, visually degraded cell contents, and characterized by dark blue to purple toluidine blue staining (Van de Velde et al., 2006). We counted visibly intact vacuoles and measured vacuole area. For histological analyses of nodule senescence, the sample sizes ranged from 341 to 1508 nodule cells sampled from 3 to 11 nodules per treatment.

We also analyzed ultrastructural features of nodule senescence; we examined evidence of infected cell senescence (defined by degradation of the plant cell contents), evidence of intact vs. ruptured symbiosomes (the latter defined by multiple breaks in the peribacteroid membrane surrounding the symbiosome), and evidence of bacteroids being released into the plant cytosol, with bacteroid data being independently sampled from 3 to 11 nodules per treatment. We quantified bacteroid population density per area as a measure of the effects of senescence on rhizobial fitness. Variation in histological and ultrastructural features was analyzed among strain treatments and among times using ANOVAs or two-tailed *t* tests with JMP Pro version 12.0 (SAS Institute, Cary, North Carolina, USA).

RESULTS

Bradyrhizobium*, but not* M. loti *genotypes, have different* in vitro *growth rates*—Previous work compared *in vitro* growth rates of the *Bradyrhizobium* genotypes and found that Br500 has the fastest doubling time (~7.25 h) followed in order by Br0, Br390, and Br380 (~7.4, ~7.7, ~8.3, respectively), all of which are significantly different from each other (Sachs et al., 2010b). Relative doubling times of the *Bradyrhizobium* strains were similar in clonal cultures and in co-cultures (Sachs et al., 2010b). Thus, there are natural differences in growth rate between the *Bradyrhizobium* genotypes that must be considered. MAFF expressing DsRed and the ineffective STM-6, in contrast, have no *in vitro* growth difference; doubling times were ~3.5 h vs. ~3.7 h, respectively (ANOVA, $F_{1, 20} = 0.057$, $P = 0.814$). There is no evidence that the STM-6 mutant is compromised for *in vitro* growth, relative to MAFF.

Nodules infected with ineffective rhizobia have evidence for accelerated senescence—*Acmispon strigosus* host plants inoculated with the effective *Bradyrhizobium* strains Br500, Br390, and Br380 possessed numerous, dark-pink root nodules and grew during the experiment, whereas those inoculated with the ineffective strain Br0 were chlorotic, possessed small, white to green nodules and did not grow, consistent with past work (Sachs et al., 2010a, b; Regus et al., 2014, 2015).

Using light microscopy, we observed that *A. strigosus* nodules infected with the most effective *Bradyrhizobium* strain (Br500) possessed infected cells with even toluidine blue staining at 5–8 wpi (Fig. 1A, B; Appendix S1B, D, F, see Supplemental Data with this article). Intact vacuoles were visible within >30% of the infected cells (Table 1). At 8 wpi, this pattern was also true for the *A. strigosus* nodules infected with the two other effective *Bradyrhizobium* strains, Br390 (Fig. 1C, D) and Br380 (Fig. 1E, F). The nodules infected with the ineffective *Bradyrhizobium* strain Br0 also had infected cells with visible vacuoles and even toluidine blue staining in nodules sampled at 5 wpi (Appendix S1A). However, by 6 wpi and 8 wpi, intact vacuoles were no longer visible within any of the infected cells of nodules infected with Br0. These nodules exhibited blotchy, uneven, blue-purple toluidine blue staining throughout their infected portions (Fig. 1G, H; Appendix S1C, E), a pattern consistent with a program of autophagic cell death initiated by rupture of the tonoplast (Van de Velde et al., 2006; van Doorn, 2011). The percentage of senescent cells in nodules infected with Br0 was striking; nearly all cells exhibited markers for senescence, relative to 0–1.5% in the other treatments (Table 1). None of the uninfected regions of any of the nodules exhibited evidence of senescence.

We also quantified and determined the average sizes of the vacuoles and cells of the nodules. At 8 wpi, the vacuoles were significantly smaller within nodules infected with Br380 (3.7 ± 0.4% of cell area), which is the least effective of these strains (Sachs et al., 2010a), compared with vacuoles with the more effective strains (Br390, 12.4 ± 0.8%; Br500, 10.3 ± 0.4%; ANOVA, $F_{2, 119} = 56.64$, $P < 0.0001$). The sizes of vacuoles in nodules infected with Br0 could not be determined at 8 wpi because there were no vacuoles that could be detected from the four nodules that we examined. Past work showed that *A. strigosus* nodule size is positively correlated with the symbiotic effectiveness of the infecting *Bradyrhizobium* strain (Regus et al., 2015). Here we found that the infected host cells of nodules varied significantly in size among different *Bradyrhizobium* strains, consistent with the mean benefit of each strain (ANOVA, $F_{3, 559} = 36.35$, $P < 0.0001$; Table 2). Interestingly, we found parallel cell size differences for interstitial cells (ANOVA, $F_{3, 560} = 127.78$, $P < 0.0001$; Table 2) and cortex cells (ANOVA, $F_{3, 559} = 66.55$, $P < 0.0001$; Table 2). In all cases, the ineffective Br0 genotype formed the smallest nodule cells.

The advantage of the *A. strigosus–Bradyrhizobium* system is the natural variation in symbiotic effectiveness among symbiont strains. Nonetheless, it has two potential confounding factors. The strains are genetically different and grow at different rates *in vitro*. Therefore, we

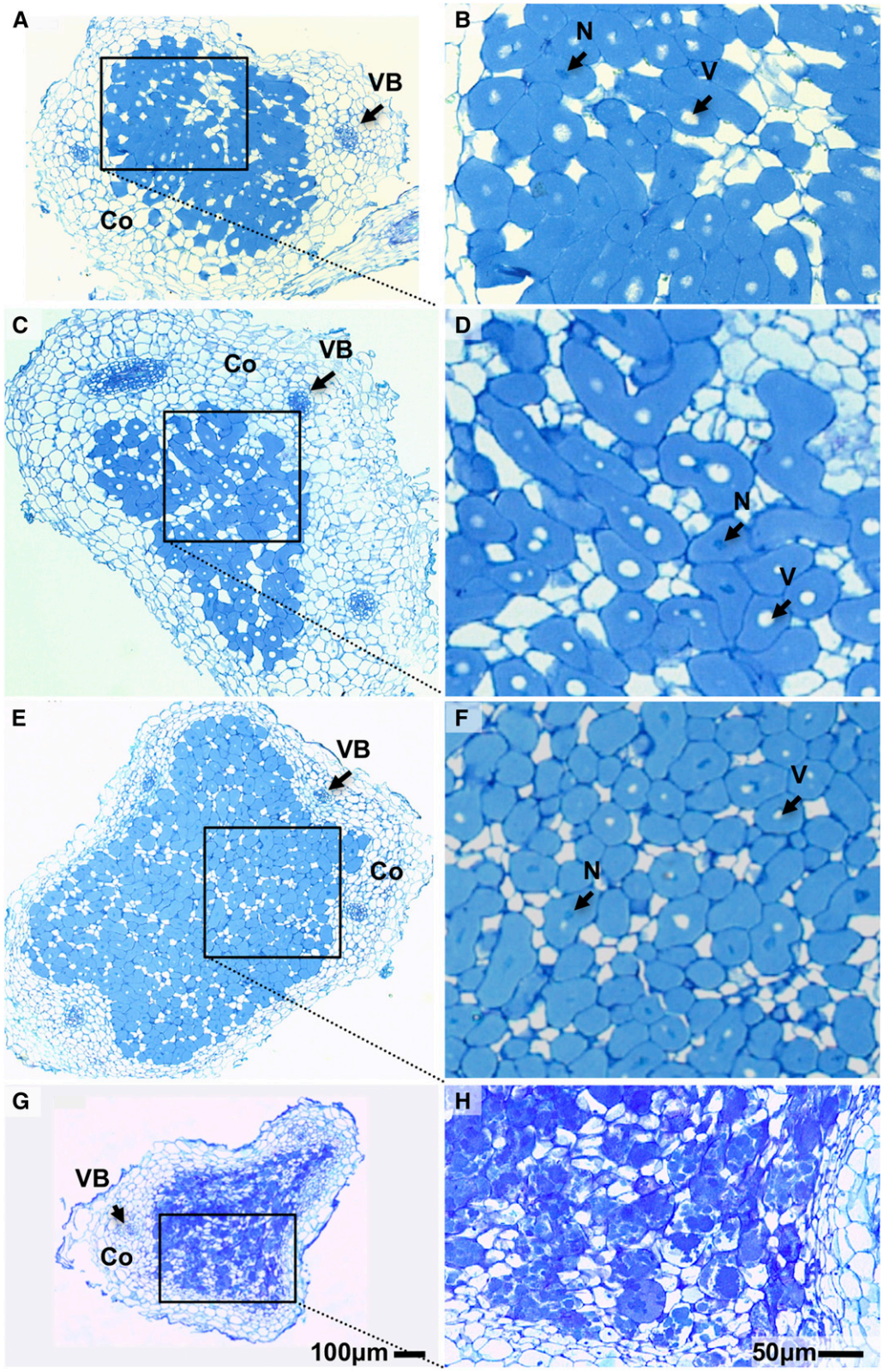

FIGURE 1 Light micrographs of thin sections of clonally infected *Acmispon strigosus* nodules at 8 weeks postinoculation viewed at 45× (A, C, E, G) and 135× magnification (B, D, F, H) and stained with toluidine blue O. Nodules are infected by effective strains Br500 (A, B), Br390 (C, D), Br380 (E, F), or the ineffective strain Br0 (G, H). *Abbreviations:* Co, cortex; VB, vascular bundles; V, vacuoles; N, nuclei. Scale bars: (A, C, E, G) 100 µm, (B, D, F, H) 50 µm.

TABLE 1. Histological markers of nodule senescence by host species and inoculation treatment.

Acmispon strigosus (8 wpi), Percentage of host cells examined (±SE)				*Lotus japonicus* (5 wpi), Percentage of total host cells examined (±SE)			
Strain (*N*, host cells)	Infected	Infected, with vacuoles	Infected, senescent	Strain	Infected	Infected, with vacuoles	Infected, senescent
Br500 (842)	75.5 ± 2.8	31.5 ± 2.1	0	MAFF (534)	53.2 ± 0.3	61.5 ± 1.5	0
Br390 (1508)	74.7 ± 2.3	43.7 ± 3.1	0	STM-6 (341)	44.6 ± 16.1	11.5 ± 2.7	57.1 ± 0
Br380 (1017)	80.4 ± 3.3	15.0 ± 1.1	1.52 ± 1.05				
Br0 (677)	72.1 ± 5.9	0 ± 0	93.5 ± 4.49				

Notes: *L. japonicus* was analyzed at 5 wpi because whole nodules began to break down after this time.

used the *L. japonicus–M. loti* system to determine whether the difference in host cell morphologies could be repeated using near-isogenic strains differing in their ability to fix nitrogen; STM-6 is derived from MAFF303099 and has an insertion in a single gene necessary for fixing nitrogen. The results were consistent between the different host–symbiont systems. *Lotus japonicus* host plants inoculated with the effective *Mesorhizobium* MAFF possessed numerous, dark-pink root nodules (Appendix S2A, arrows) and grew to maturity producing flowers and fruits during the experiment, whereas those inoculated with the Fix$^-$ mutant, STM-6, were chlorotic, possessed small, white to green nodules (Appendix S2B, arrows) and did not grow. *Lotus japonicus* nodule cells with the effective MAFF strain had intact vacuoles and even toluidine blue staining at 3 and 7 wpi (Fig. 2A, C), as seen in nodules of *A. strigosus* with effective rhizobia. In contrast, *L. japonicus* nodule cells with the Fix$^-$ mutant STM-6 initially exhibited infected cells with even toluidine straining at 3wpi and with visible vacuoles (Fig. 2B), but by 5 wpi we observed a lower percentage of visible intact vacuoles and a substantially higher percentage of cells with blotchy, uneven toluidine staining, consistent with autophagic cell death (Table 1; Fig. 2D).

At 3 wpi, the vacuoles were significantly smaller within nodules infected by STM-6 than in those infected with MAFF (STM-6, 3.7 ± 0.30% of cell area; MAFF, 9.9 ± 0.78%; *t* test, t = 56.78, df = 39, $P < 0.0001$). With respect to average cell area in *L. japonicus* nodules, those at 3 wpi and 5 wpi and infected with STM-6 were smaller than age-matched nodules infected with MAFF (Table 2). Interstitial and cortex cells were also smaller in nodules with STM-6.

Using transmission electron microscopy, we compared ultrastructural features of effective and ineffective clonal infections. At times between 7–9 wpi, *A. strigosus* nodules infected with the effective *Bradyrhizobium* strain Br500 had infected host cells with intact symbiosomes. The density of intact bacteroids per area within nodules increased over the observed period of 7–9 wpi (Table 3; Fig. 3A–C). *Acmispon strigosus* nodules infected with the ineffective *Bradyrhizobium* strain Br0 at 4 wpi had intact symbiosomes. By 7 wpi, the peribacteroid membranes that surround the symbiosomes within nodules infected with Br0 were ruptured, and the bacteroids appeared to be present in the cytosol. By 9 wpi, nodules infected with Br0 had no visible intact symbiosomes. The density of bacteroids with Br0 decreased rapidly over the time investigated, consistent with bacteroid death and host selection against ineffective bacteroids (Table 3).

Lotus japonicus nodules infected with MAFF had infected cells with intact symbiosomes at 3–5 wpi (Fig. 2E, G). The symbiosomes in these nodules each housed ~1 bacteroid. *Lotus japonicus* nodules infected with STM-6 had intact symbiosomes that housed 1–2 bacteroids each (at 3 wpi). However, by 5 wpi, many symbiosomes were observed to be ruptured (Fig. 2F, H). Densities of intact bacteroids were initially similar in MAFF and STM-6 infected nodules, and although both dropped in density by 5 wpi, the bacteroid density was significantly lower for STM-6 than for MAFF (5 wpi; *t* test, $t = 17.82$, df = 18, $P = 0.0006$), consistent with host selection against ineffective bacteroids (Table 3).

Sanctions are imposed at the level of the host cell—We next asked whether host selection against ineffective bacteroids is imposed on a whole nodule or cell level. *Acmispon strigosus* hosts that were coinoculated with one of the effective *Bradyrhizobium* strains (i.e., Br500 or Br390) plus the ineffective strain Br0 had nodules with mixed histological features. Under light microscopy, a subset of the infected host cells had features similar to those of nodules singly infected with an effective strain, while another subset resembled those infected singly with Br0 (Figs. 1, 4). Moreover, the subsets of host cells were spatially sectored into different regions of the nodule (Fig. 4). In plants coinoculated with

TABLE 2. Cell area in nodules by host species, cell type, and inoculation treatment.

Acmispon strigosus (8 wpi)				*Lotus japonicus* (3,5 wpi)			
Cell type	Strain (*N*, host cells)	Cell area ($\mu m^2 \times 10^3 \pm SE$)	ANOVA	Cell type	Strain, Time, (*N*, host cells)	Cell area ($\mu m^2 \times 10^3 \pm SE$)	*t* test
Infected	Br500 (150)	2.52 ± 0.085	$F = 36.34$	Infected	MAFF, 3 wpi (40)	5.35 ± 0.049	$t = 82.5$
	Br390 (200)	2.07 ± 0.074	$P < 0.0001$		STM-6, 3 wpi (40)	0.84 ± 0.005	$P < 0.0001$
	Br380 (150)	1.65 ± 0.085			MAFF, 5 wpi (40)	3.42 ± 0.210	$t = 120.4$
	Br0 (60)	1.02 ± 0.130			STM-6, 5 wpi (40)	0.88 ± 0.009	$P < 0.0001$
Interstitial	Br500 (150)	1.04 ± 0.043	$F = 127.78$	Interstitial	MAFF, 3 wpi (40)	0.96 ± 0.080	$t = 62.2$
	Br390 (200)	1.18 ± 0.034	$P < 0.0001$		STM-6, 3 wpi (40)	0.31 ± 0.002	$P < 0.0001$
	Br380 (150)	0.48 ± 0.026			MAFF, 5 wpi (40)	0.28 ± 0.002	$t = 2.8$
	Br0 (60)	0.11 ± 0.014			STM-6, 5 wpi (40)	0.23 ± 0.002	$P = 0.097$
Cortex	Br500 (150)	1.42 ± 0.067	$F = 66.55$	Cortex	MAFF, 3 wpi (40)	1.37 ± 0.120	$t = 53.0$
	Br390 (200)	1.74 ± 0.054	$P < 0.0001$		STM-6, 3 wpi (40)	0.47 ± 0.003	$P < 0.0001$
	Br380 (150)	0.88 ± 0.056			MAFF, 5 wpi (40)	0.61 ± 0.003	$t = 5.8$
	Br0 (60)	0.48 ± 0.040			STM-6, 5 wpi (40)	0.50 ± 0.003	$P = 0.018$

Notes: ANOVAs were used to compare among strain treatments on *A. strigosus*, and *t*-tests were used to compare between the strain treatments on *L. japonicus*.

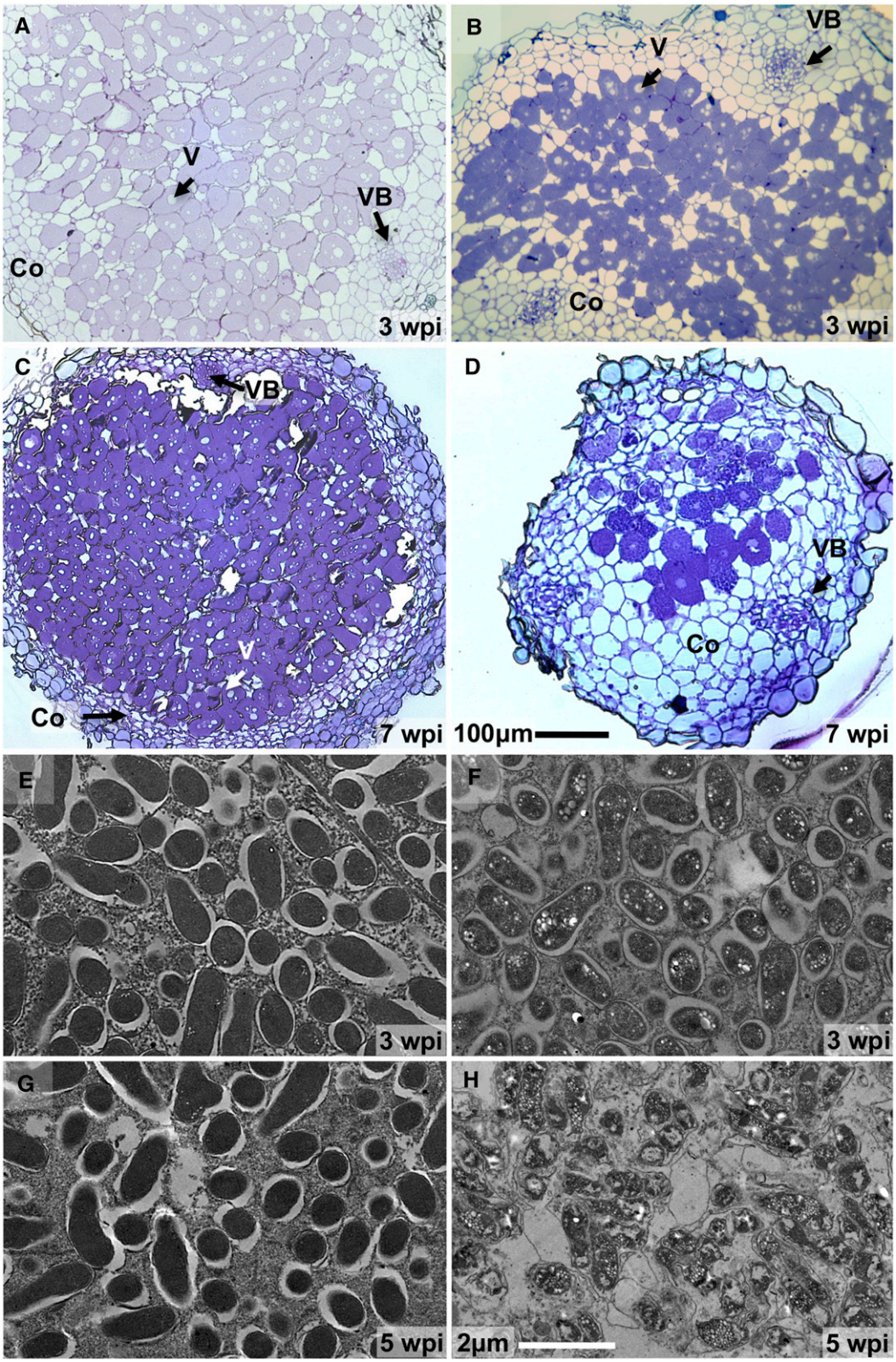

FIGURE 2 Light micrographs (A–D, stained with toluidine blue O) and TEM images (E–H) of clonally infected *Lotus japonicus* nodules at 3 weeks postinoculation (wpi) (A, B, E, F), 5 wpi (G, H), and 7 wpi (C, D). Nodules are infected by the effective wild-type strain MAFF (A, C, E, G), or the ineffective mutant strain STM-6 (B, D, F, H). *Abbreviations:* Co, cortex; VB, vascular bundles; V, vacuoles. Scale bars: (A–D) 100 µm, (E–H) 2 µm.

TABLE 3. Bacteroid density and counts of bacteroids per symbiosome over time.

Acmispon strigosus					*Lotus japonicus*		
	Bacteroid density/$\mu m^2 \pm$ SE (*N*)					Bacteroid density/$\mu m^2 \pm$ SE (*N*)	
Strain	4 wpi	7 wpi	8 wpi	9 wpi	Strain	3 wpi	5 wpi
Br500	—	0.86 ± 0.05 (4)	0.82 ± 0.05 (3)	1.69 ± 0.16 (3)	MAFF	0.93 ± 0.11 (10)	0.70 ± 0.06 (10)
Br0	0.96 ± 0.02 (5)	0.92 ± 0.11 (4)	0.48 ± 0.04 (4)	0.46 ± 0.25 (4)	STM-6	1.04 ± 0.21 (11)	0.37 ± 0.23 (10)

Br500 and Br0, most of the infected nodule cells exhibited even toluidine blue staining and large intact vacuoles, consistent with features associated with Br500. But there were also small clusters of host cells with blotchy staining that lacked intact vacuoles, consistent with features associated with host cells infected with Br0 (Fig. 4A, B). A similar pattern of sectoring was observed in nodules from plants coinoculated with Br390 and Br0 (Fig. 4C, D). Nodule sectoring was not previously observed in the nodules from singly infected plants (Figs. 1, 2). Sectoring was only observed in *A. strigosus* plants that received mixed inoculations and present in 12 of 88 observed nodules. The 14% of sectored nodules is consistent with empirically determined nodule coinfection rates of *A. strigosus* that was previously quantified using the same *Bradyrhizobium* genotypes (Sachs et al., 2010b; Regus et al., 2014). Importantly, the sectoring suggests host sanctions may be imposed at a smaller scale than the whole nodule.

We also observed that *A. strigosus* nodules showed ultrastructural evidence of sectoring in hosts that received mixed inoculations of *Bradyrhizobium* strains Br500 and Br0. Transmission electron micrographs taken at 7, 8, and 9 wpi revealed a subset of infected cells that exhibited intact symbiosomes, consistent with strain Br500 ultrastructural features. Similar to observations based on light microscopy, coinoculated nodules had another subset of infected cells with morphological features consistent with programmed cell death. This second subset of cells exhibited symbiosomes with ruptured peribacteroid membranes and with bacteroids released into the cytosol, consistent with nodules infected with Br0 (Fig. 3H, I). By 9 wpi, a subset of plant cells appeared senescent, within which all the cellular contents appeared to be degraded and with no signs of surviving bacteroids, again consistent with features associated with Br0 (Fig. 3J). In all, the ultrastructural observations on coinoculated nodules suggest sanctions are enacted at a scale smaller than the nodule. The rapid senescence of a spatially restricted subset of infected nodule cells suggests that *A. strigosus* hosts can selectively induce programmed cell death of nodule cells that are not generating sufficient symbiotic benefits to the host.

Sanctioned host cells are infected with ineffective rhizobia—To demonstrate that sanctions are targeted specifically to host cells housing ineffective strains, we coinoculated *L. japonicus* with MAFF expressing DsRed and the Fix^- STM-6 expressing GFP, and used confocal imaging to associate host cell morphologies to the infected bacterial genotype. The two different ratios of MAFF to STM-6, 3:7 and 1:19 used had no obvious effects on nodule histology. *Lotus japonicus* plants individually infected with MAFF (DsRed) and Fix^- STM-6 (GFP) were also included as controls. Fluorescent bacterial cells could be observed at 8 wpi (MAFF) and at 4 wpi (STM-6) in intact nodule cells, consistent with the light microscopy data (Fig. 5A, B; Appendix S3).

In coinoculated *L. japonicus* hosts, we observed sectored nodules in 5 of 12 nodules in the 3:7 MAFF–STM-6 treatment and 11 of the 20 nodules in the 1:19 treatment. At 4 wpi, the red and green fluorescence was spatially sectored in the nodules, and the infected plant cells appeared to be intact (Fig. 5C; Appendix S3). At 7 wpi, fluorescent bacteria were still separated into different sectors of the nodule, but there were clear morphological changes that were only associated with sectors of GFP-expressing STM-6. Their host cells showed evidence of senescence and whole-cell rupture, with GFP-expressing bacteroids showing evidence for having been released from host cells and localized in the intercellular spaces (Fig. 5D–F). Host cells that were only associated with DsRed (MAFF) did not show any of these signs of senescence. Some host cells appeared to contain a mix of GFP and DsRed (Fig. 5E, F), but this may be an artifact of the depth of field. These observations are consistent with the model that sanctions function primarily against ineffective bacteria and that sanctions occur at the level of the single host cell.

DISCUSSION

We tested the model that senescence induced in legume nodules can target ineffective rhizobia in host species with determinate nodule development. First, we examined features of singly infected host cells to gain insights into the mechanism of sanctions. When infected with ineffective rhizobia, *A. strigosus* and *L. japonicus* formed nodules with features that others previously ascribed to a program of autophagic cell death, but we hypothesize as induced cellular senescence (van Doorn, 2011). Features were visible at 5–6 wpi and included (1) blotchy, uneven toluidine blue staining, (2) collapsed or absent vacuoles, and (3) ruptured symbiosomes releasing bacteroids into the cytosol and resulting in low populations of ineffective bacteroids (Figs. 1–3, Tables 1, 3; Appendix S1). In contrast, nodules of *A. strigosus* and *L. japonicus* with effective rhizobia featured infected cells that had (1) even toluidine blue staining that persisted over a significant period of nodule development (i.e., 5–9 wpi), (2) intact vacuoles (Figs. 1–3; Appendix S1), and (3) maintained intact symbiosomes with relatively stable bacteroid populations (Table 3). These latter features are typical of effective nodules in legumes with determinate nodule development (Chua et al., 1985; Banba et al., 2001; Schumpp and Deakin, 2010; Thapanapongworakul et al., 2010; Chungopast et al., 2014). The features associated with the hypothesized induced cellular senescence appeared to initiate slightly earlier in *L. japonicus* hosts (~5 wpi) compared to *A. strigosus* (~6 wpi) consistent with the early-flowering phenotype and faster development of the *L. japonicus* MG-20 accession (Kawaguchi, 2000). In both plant species studied here, only plants that were inoculated with non-nitrogen-fixing strains had substantial numbers of infected cells undergoing the proposed process of induced senescence. The patterns of reduced bacteroid populations support the possibility that cellular senescence is responsible for sanctioning the ineffective rhizobia. The specific trigger that induces senescence remains unknown, but one hypothesis is that senescence is triggered by antioxidants that are coupled to low carbon to nitrogen ratios inside the nodule (Puppo et al., 2005).

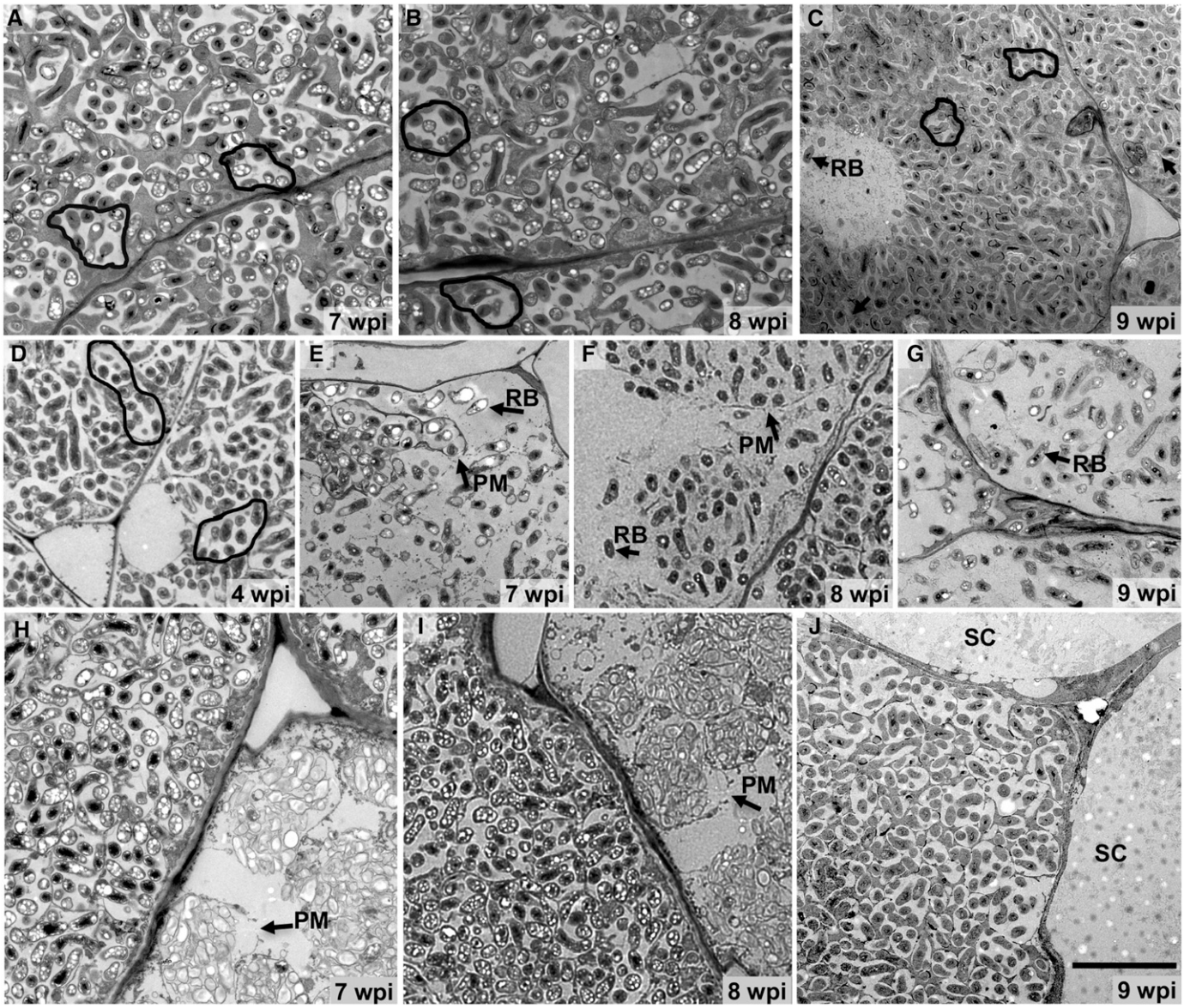

FIGURE 3 TEM images from *Acmispon strigosus* plants inoculated with effective strain Br500 (A–C), ineffective strain Br0 (D–G), or both (H–J), sampled at 4–9 weeks postinoculation (wpi). Nodules infected by effective strain Br500 exhibit intact symbiosomes (black lines) from 7–9 wpi (A–C) containing ~5–10 bacteroids and with evidence of released bacteroids (RB) only at ~9 wpi (C). Nodules infected by the ineffective strain Br0 initially exhibit intact symbiosomes at 4 wpi (D) containing 10–20 bacteroids; however, ruptured symbiosomes with broken pieces of peribacteroid membranes (PM) and released bacteroids are visible at 7–9 wpi (E–G). At 9 wpi, nodules infected by Br0 are devoid of intact symbiosomes (G). Nodules of coinoculated plants exhibit sectored patterns consistent with coinfection by both strains: some cells exhibit intact symbiosomes containing 5–10 bacteroids, consistent with strain Br500, whereas neighboring cells exhibit symbiosomes with 10–20 bacteroids each and with broken peribacteroid membranes, consistent with strain Br0 (H–J). At 9 wpi, nodules of coinoculated plants exhibit some senesced cells (SC) devoid of any intracellular structures (J). Scale bars: 5 μm.

A second element of the model that was tested was the cell-autonomous nature of legume sanctioning. Nodules of *A. strigosus* and *L. japonicus* exhibited sectored histological features when hosts were coinoculated with both effective and ineffective rhizobia. Using bacteria expressing fluorescent proteins, we were able to demonstrate that different genotypes of bacteria occupied different sectors within nodules and that only the ineffective genotypes were associated with features of cellular senescence (Fig. 5). Sectoring has been previously observed in other legume species when hosts were inoculated with multiple rhizobial strains, but were characterized independent of sanctioning. For instance, when soybean was coinoculated with an effective *Bradyrhizobium* and a Fix^- mutant, the nodules formed sectors with pink and white colors, indicative of leghemoglobin being localized to specific regions of the nodule (Hahn and Studer, 1986). Likewise, when alfalfa was coinoculated with GFP- and RFP-expressing *Sinorhizobium*, the fluorescent colors often sectored within coinfected nodules (Gage, 2002).

The efficiency of sanctioning is predicted to depend on the ability of the host plant to spatially structure symbionts, thus separating effective from ineffective partners (Denison, 2000; West et al., 2002a, b;

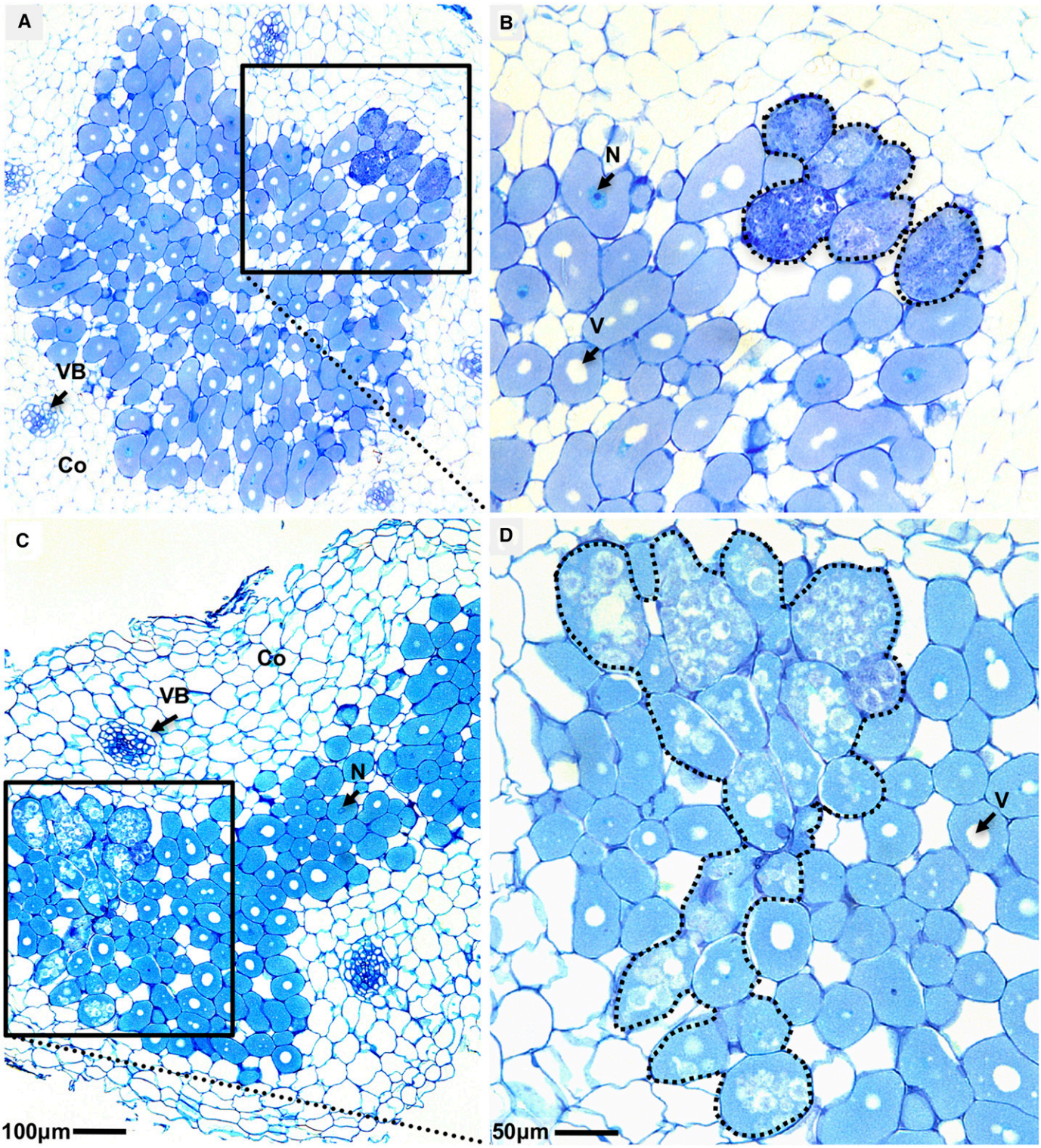

FIGURE 4 Light micrographs of thin sections of *Acmispon strigosus* nodules from plants with mixed-strain inoculations of strain Br0 and Br500 (A, B) or Br0 and Br390 (C, D) at 8 weeks postinoculation, stained with toluidine blue O. Most infected cells exhibit histological features consistent with effective strains, including even staining, and intact vacuoles (V) and nuclei (N). However, localized subsets of infected plant cells have morphologies consistent with ineffective strain Br0 (B, D; dotted black line), with blotchy staining and evidence of ruptured vacuoles. *Abbreviations:* Co, cortex; VB, vascular bundles. Scale bars: (A, C) 100 µm, (B, D) 50 µm.

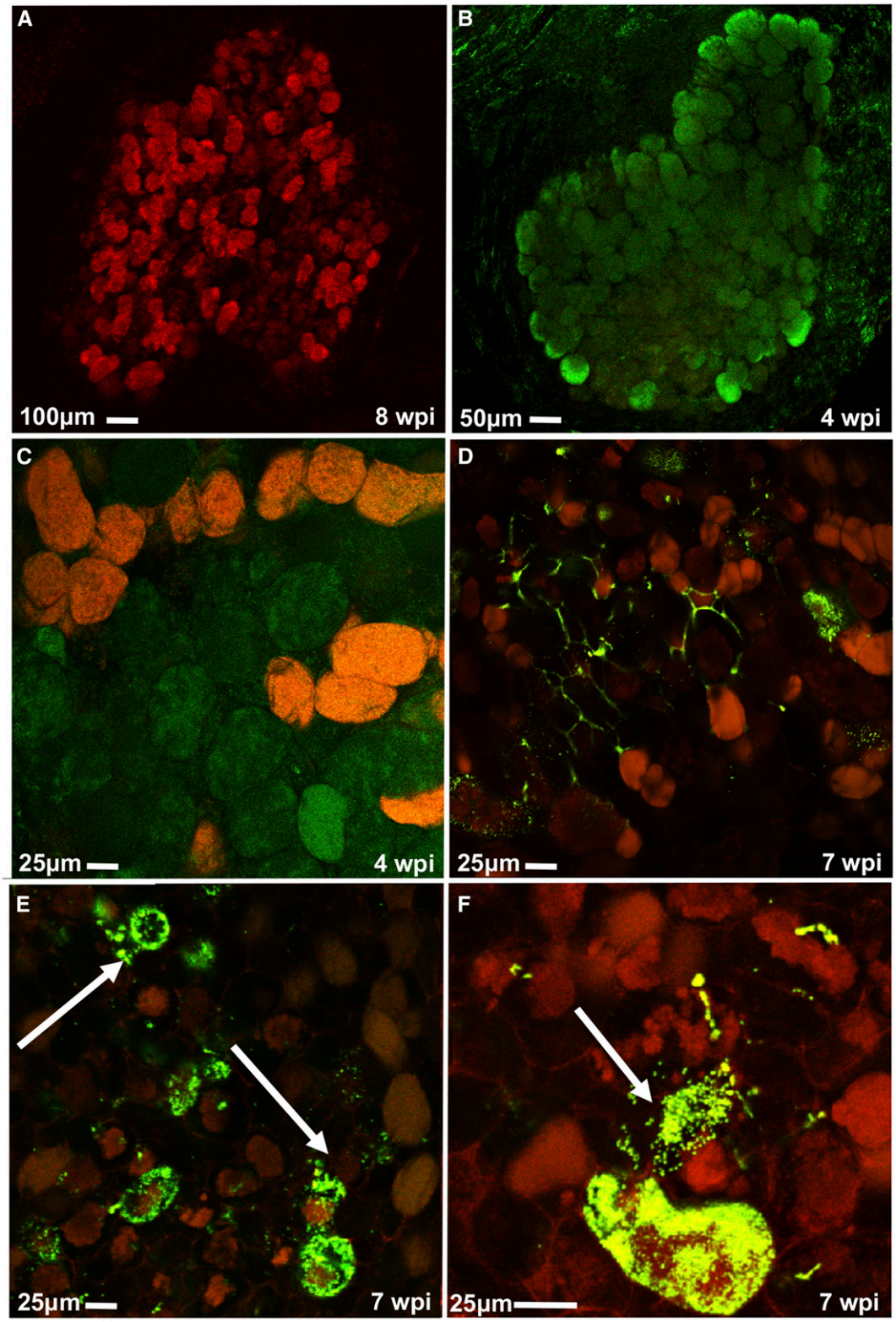

FIGURE 5 Laser scanning confocal imaging of *Lotus japonicus* nodules infected by MAFF-DsRed (A), the Fix$^-$ mutant STM-6-GFP (B), or both (C–F). (A) Nodule cells infected by MAFF-DsRed appear red and intact at 8 weeks postinoculation (wpi); (B) nodule cells infected by STM-6 appear green and intact at 4 wpi. (C–F) Four different coinfected nodules each show a sectored pattern with neighboring cells dominated by different *Mesorhizobium loti* strains, with no signs of senescence at 4 wpi (C). However, only nodules cells associated with GFP fluorescence exhibited signs of senescence at 7 wpi (D–F), in some cases, with ruptured cells that appeared to be releasing GFP-expressing rhizobia into the intercellular spaces (white arrows). A magnified version of a ruptured cell is shown in (F). Scale bars: (A) 100 µm, (B) 50 µm, (C–F) 25 µm. Grayscale versions of these images are also provided in Appendix S3.

Sachs et al., 2011b). A simulation model predicted that nodule sectoring can be a stochastic process, assuming that multiple rhizobial strains are present in the infection thread, rhizobial movement is limited *in planta,* and there is relatively little variation in rhizobial *in planta* growth rates (Gage, 2002). We therefore suggest that the host plant does not necessarily actively enforce sectoring as a part of the sanctioning process. Rather, we suggest that cell autonomous sanctions can be imposed because infection naturally sectors the infecting symbiont population. The evolutionary importance of nodule sectoring logically depends on the frequency of mixed nodule infections in nature and possibly fitness differences within symbiont populations.

The cell-autonomous, induced cellular senescence mechanism meets three minimal criteria necessary for the sanctions to be efficacious in coinfected nodules: the mechanism of sanctions that we described here (I) distinguishes between effective and ineffective rhizobial genotypes and becomes instigated only in the presence of ineffective rhizobia, (II) sanctions ineffective rhizobial genotypes within coinfected nodules to decrease the fitness of only the ineffective rhizobia and appears cell-autonomous within coinfected nodules, and (III) does not disrupt the integrity of the entire nodule and is demonstrably localized to specific regions of the nodule. Diverse legumes express sanctions traits that reduce fitness of ineffective rhizobial genotypes, including host taxa with determinate (Singleton and Stockinger, 1983; Kiers et al., 2003; Sachs et al., 2010b) and indeterminate nodule development (Simms et al., 2006; Oono et al., 2011). Whether the cell-autonomous model applies to legumes with indeterminate nodules, in which nitrogen-fixing bacteroids are terminally differentiated and spatially separated from their undifferentiated reproductive clonemates, is unknown.

Several mechanisms have been previously proposed for sanctions, but none appear to be effective in mixed nodule infections. Withholding plant carbon is a possible mechanism of sanctions (Oono et al., 2009). But in many plant species carbon is passively diffused in nodules, violating criterion II (White et al., 2007; Vance, 2008; Oono et al., 2009). Regulating the availability of certain amino acids is another potential form of sanctions (Prell et al., 2009; Reid et al., 2011). However, evidence suggested that bacteroids become dependent on the host for amino acids conditional upon symbiosis, not as a consequence of the services provided (violates criterion I) (Prell et al., 2009; Reid et al., 2011). Legumes also control nodule formation to optimize nitrogen fixation in relation to carbon demands, termed autoregulation of nodulation (Reid et al., 2011). But autoregulation occurs at an early step in nodulation and is not entirely dependent on nitrogen fixation in the nodule (Reid et al., 2011), violating criterion I. Legumes of the Inverted Repeat-lacking Clade (Faboideae) secrete antimicrobial peptides to trigger terminal differentiation of bacteroids, so that these bacterial cells cannot escape the nodule (Maruya and Saeki, 2010; Van de Velde et al., 2010; Wang et al., 2010; Haag et al., 2011). But undifferentiated rhizobia also persist in these nodules and are not subject to antimicrobial control (violates criterion II). Finally, the dominant model of sanctions proposes that the host can decrease oxygen flux to whole nodules that contain ineffective rhizobia (Sheehy et al., 1983; Kiers et al., 2003), but to date there is no known mechanism for control over oxygen flux to individual plant cells, violating criterion III.

Evolutionary models have predicted that even low levels of nodule coinfection might lead to the destabilization of nitrogen fixation (West et al., 2002a, b; Friesen, 2012). The frequency in which hosts are coinfected remains poorly understood. Genotyping of nodules from field-grown plants suggest that the frequency of mixed infections might be as low as 1–3% (Simms et al., 2006; van Berkum et al., 2012). But these genetic studies lacked sufficient resolution to discriminate closely related rhizobia and their potentially wide-ranging symbiotic phenotypes (Sachs et al., 2010a, 2011a). Furthermore, in the field, sanctions will inevitably reduce the fitness of coinfected ineffective strains and will obscure mixed infections. In the laboratory, mixed infection nodules can be easily generated (Johnston and Beringer, 1975; Labandera and Vincent, 1975; Brockwell et al., 1977; Bromfield and Jones, 1980; Amarger, 1981; Hahn and Studer, 1986; Gage, 2002; Heath and Tiffin, 2009; Sachs et al., 2010b; Checcucci et al., 2016). But these experiments might overestimate the frequency of mixed nodule infections because plants are often inoculated with unnaturally high concentrations of rhizobia (Mathu et al., 2012; Tang et al., 2012).

The evolutionary origins of sanctions have been a topic of intense controversy that relates to the mechanistic bases of these traits (Weyl et al., 2010; Kiers et al., 2011; Frederickson, 2013). One hypothesis is that sanctions derive from conserved root-foraging traits whereby plants allocate carbon to tissues based on local nitrogen concentration (Weyl et al., 2010; Frederickson, 2013). Given the presumption that root foraging traits are anciently conserved in plants (Kembel and Cahill, 2005), authors have suggested that sanctions predate the origins of the legume–rhizobium symbiosis and thus could not have evolved in response to ineffective rhizobia (Weyl et al., 2010; Frederickson, 2013). However, several inconsistencies with this model have become apparent with recent data. First, legumes can efficiently sanction ineffective rhizobia even when exposed to high nitrogen concentrations in soil, suggesting that sanctions can occur independently of the response to extrinsic soil nutrients (Kiers et al., 2006; Regus et al., 2014; Grillo et al., 2016). Moreover, data herein and elsewhere suggest that sanctions can occur even when nodules contain mixed strain infections (Sachs et al., 2010b; Regus et al., 2014), suggesting that sanctions can respond to cellular differences in tissue nitrogen concentration, which might not be expected based on our current understanding of root-foraging traits (Kembel and Cahill, 2005). All of these data suggest that sanctions are a response to the evolution of root associates that exploit plant resources without reciprocation.

Diverse bacteria provide plant hosts with a broad array of resources and services including enhanced growth, resistance to pathogens, and tolerance to drought and other stressors (Mueller and Sachs, 2015). In most of these cases, plants acquire bacterial symbionts from the environment; hence, seedlings must select favorable symbiont genotypes to associate with from the diverse array of bacteria present in the soil (Sachs et al., 2011b). As demonstrated in this study, plants may also selectively punish less-desirable genotypes after they have been acquired. Our increasing understanding of the mechanistic bases of sanctions traits and their genomic drivers will shed light upon how symbioses evolved, how they are stabilized over evolutionary time, and how we can leverage these plant traits for our own utility.

ACKNOWLEDGEMENTS

We thank Yifan Lii, David Carter, Darleen DeMason, and the Central Facility for Advanced Microscopy and Microanalysis at UCR for assistance with microscopy and plant tissue preparation. We also thank Camille Wendlandt, Kelsey Gano, and anonymous reviewers for helpful comments on the manuscript. This work was funded by NSF DEB 1150278 to J.L.S., E.A.S. was supported by USDA (U. S. Department of Agriculture) NIFA (National Institute of Food and Agriculture) post-doctoral fellowship #2013-67012-21139, and J.H.C was supported in part by USDA NIFA grant 2014-51181-22384.

AUTHOR CONTRIBUTIONS

J.U.R., K.W.Q., J.H.C., and J.L.S. designed the experiments. J.U.R., K.W.Q., M.R.O., R.S., E.A.S., and J.L.S. performed the experiments and collected data. J.U.R., J.H.C., and J.L.S. wrote the manuscript.

LITERATURE CITED

Allan, G. J., and J. M. Porter. 2000. Tribal delimitation and phylogenetic relationships of Loteae and Coronilleae (Faboideae: Fabaceae) with special reference to *Lotus*: Evidence from nuclear ribosomal ITS sequences. *American Journal of Botany* 87: 1871–1881.

Amarger, N. 1981. Competition for nodule formation between effective and ineffective strains of *Rhizobium meliloti*. *Soil Biology & Biochemistry* 13: 475–480.

Banba, M., A. B. M. Siddique, H. Kouchi, K. Izui, and S. Hata. 2001. *Lotus japonicus* forms early senescent root nodules with *Rhizobium etli*. *Molecular Plant-Microbe Interactions* 14: 173–180.

Brockwell, J., E. A. Schwinghamer, and R. R. Gault. 1977. Ecological studies of root-nodule bacteria introduced into field environments. V. A critical examination of stability of antigenic and streptomycin-resistance markers for identification of strains of *Rhizobium trifolii*. *Soil Biology & Biochemistry* 9: 19–24.

Bromfield, E. S. P., and D. G. Jones. 1980. A strain marker in *Rhizobium trifolii* based on the absorption of congo red. *Zentralblatt fur Bakteriologie, Parasitenkunde, Infektionskrankheiten und Hygiene. Zweite Naturwissenschaftliche Abteilung: Mikrobiologie der Landwirtschaft der Technologie und des Umweltschutzes* 135: 290–295.

Burdon, J. J., A. H. Gibson, S. D. Searle, M. J. Woods, and J. Brockwell. 1999. Variation in the effectiveness of symbiotic associations between native rhizobia and temperate Australian *Acacia*: Within-species interactions. *Journal of Applied Ecology* 36: 398–408.

Chang, J. H., J. M. Urbach, T. F. Law, L. W. Arnold, A. Hu, S. Gombar, S. R. Grant, et al. 2005. A high-throughput, near-saturating screen for type III effector genes from *Pseudomonas syringae*. *Proceedings of the National Academy of Sciences, USA* 102: 2549–2554.

Checcucci, A., E. Azzarello, M. Bazzicalupo, M. Galardini, A. Lagomarsino, S. Mancuso, L. Marti, et al. 2016. Mixed nodule infection in *Sinorhizobium meliloti–Medicago sativa* symbiosis suggests the presence of cheating behavior. *Frontiers in Plant Science* 7: 835.

Chua, K. Y., C. E. Pankhurst, P. E. MacDonald, D. H. Hopcroft, B. D. W. Jarvis, and D. B. Scott. 1985. Isolation and characterization of transposon Tn5-induced symbiotic mutants of *Rhizobium loti*. *Journal of Bacteriology* 162: 335–343.

Chungopast, S., P. Thapanapongworakul, H. Matsuura, D. Tan Van, T. Asahi, K. Tada, S. Tajima, and M. Nomura. 2014. Glutamine synthetase I-deficiency in *Mesorhizobium loti* differentially affects nodule development and activity in *Lotus japonicus*. *Journal of Plant Physiology* 171: 104–108.

Collins, M. T., J. E. Thies, and L. K. Abbott. 2002. Diversity and symbiotic effectiveness of *Rhizobium leguminosarum* bv. *trifolii* isolates from pasture soils in south-western Australia. *Australian Journal of Soil Research* 40: 1319–1329.

Degtjareva, G. V., T. E. Kramina, D. D. Sokoloff, T. H. Samigullin, C. M. Valiejo-Roman, and A. S. Antonov. 2006. Phylogeny of the genus *Lotus* (Leguminosae, Loteae): Evidence from nrITS sequences and morphology. *Canadian Journal of Botany* 84: 813–830.

Denison, R. F. 2000. Legume sanctions and the evolution of symbiotic cooperation by rhizobia. *American Naturalist* 156: 567–576.

Denison, R. F., and E. T. Kiers. 2004. Lifestyle alternatives for rhizobia: Mutualism, parasitism, and forgoing symbiosis. *FEMS Microbiology Letters* 237: 187–193.

Denton, M. D., D. R. Coventry, W. D. Bellotti, and J. G. Howieson. 2000. Distribution, abundance and symbiotic effectiveness of *Rhizobium leguminosarum* bv. *trifolii* from alkaline pasture soils in South Australia. *Australian Journal of Experimental Agriculture* 40: 25–35.

Devine, T. E., and L. D. Kuykendall. 1996. Host genetic control of symbiosis in soybean (*Glycine max* L.). *Plant and Soil* 186: 173–187.

Devine, T. E., L. D. Kuykendall, and J. J. O'Neill. 1990. The *Rj4* allele in soybean represses nodulation by chlorosis-inducing bradyrhizobia classified as DNA homology group II by antibiotic resistance profiles. *Theoretical and Applied Genetics* 80: 33–37.

Frederickson, M. E. 2013. Rethinking mutualism stability: Cheaters and the evolution of sanctions. *Quarterly Review of Biology* 88: 269–295.

Friesen, M. L. 2012. Widespread fitness alignment in the legume–*Rhizobium* symbiosis. *New Phytologist* 194: 1096–1111.

Friesen, M. L., and A. Mathias. 2010. Mixed infections may promote diversification of mutualistic symbionts: Why are there ineffective rhizobia? *Journal of Evolutionary Biology* 23: 323–334.

Gage, D. J. 2002. Analysis of infection thread development using GFP- and DsRed-expressing *Sinorhizobium meliloti*. *Journal of Bacteriology* 184: 7042–7046.

Gogorcena, Y., A. J. Gordon, P. R. Escuredo, F. R. Minchin, J. F. Witty, J. F. Moran, and M. Becana. 1997. N_2 fixation, carbon metabolism, and oxidative damage in nodules of dark-stressed common bean plants. *Plant Physiology* 113: 1193–1201.

González, E. M., P. M. Aparicio-Tejo, A. J. Gordon, F. R. Minchin, M. Royuela, and C. Arrese-Igor. 1998. Water-deficit effects on carbon and nitrogen metabolism of pea nodules. *Journal of Experimental Botany* 49: 1705–1714.

Grillo, M. A., J. R. Stinchcombe, and K. D. Heath. 2016. Nitrogen addition does not influence pre-infection partner choice in the legume–rhizobium symbiosis. *American Journal of Botany* 103: 1763–1770.

Gubry-Rangin, C., M. Garcia, and G. Béna. 2010. Partner choice in *Medicago truncatula–Sinorhizobium* symbiosis. *Proceedings of the Royal Society, B, Biological Sciences* 277: 1947–1951.

Haag, A. F., M. Baloban, M. Sani, B. Kerscher, O. Pierre, A. Farkas, R. Longhi, et al. 2011. Protection of *Sinorhizobium* against host cysteine-rich antimicrobial peptides is critical for symbiosis. *PLoS Biology* 9: e1001169.

Hahn, M., and D. Studer. 1986. Competitiveness of a *nif*⁻ *Bradyrhizobium japonicum* mutant against the wild-type strain. *FEMS Microbiology Letters* 33: 143–148.

Handberg, K., and J. Stougaard. 1992. *Lotus japonicus*, an autogamous, diploid legume species for classical and molecular genetics. *Plant Journal* 2: 487–496.

Heath, K. D., and P. Tiffin. 2009. Stabilizing mechanisms in a legume–rhizobium mutualism. *Evolution* 63: 652–662.

Johnston, A. W. B., and J. E. Beringer. 1975. Identification of rhizobium strains in pea root nodules using genetic markers. *Journal of General Microbiology* 87: 343–350.

Jones, K. M., H. Kobayashi, B. W. Davies, M. E. Taga, and G. C. Walker. 2007. How rhizobial symbionts invade plants: The *Sinorhizobium–Medicago* model. *Nature Reviews. Microbiology* 5: 619–633.

Kawaguchi, M. 2000. *Lotus japonicus* 'Miyakojima' MG-20: An early-flowering accession suitable for indoor handling. *Journal of Plant Research* 113: 507–509.

Kembel, S. W., and J. F. Cahill Jr. 2005. Plant phenotypic plasticity belowground: A phylogenetic perspective on root foraging trade-offs. *American Naturalist* 166: 216–230.

Kiers, E. T., R. F. Denison, A. Kawakita, and E. A. Herre. 2011. The biological reality of host sanctions and partner fidelity. *Proceedings of the National Academy of Sciences, USA* 108: E7.

Kiers, E. T., R. A. Rousseau, and R. F. Denison. 2006. Measured sanctions: Legume hosts detect quantitative variation in rhizobium cooperation and punish accordingly. *Evolutionary Ecology Research* 8: 1077–1086.

Kiers, E. T., R. A. Rousseau, S. A. West, and R. F. Denison. 2003. Host sanctions and the legume–rhizobium mutualism. *Nature* 425: 78–81.

Labandera, C. A., and J. M. Vincent. 1975. Competition between an introduced strain and native Uruguayan strains of *Rhizobium trifolii*. *Plant and Soil* 42: 327–347.

Maekawa, T., M. Maekawa-Yoshikawa, N. Takeda, H. Imaizumi-Anraku, Y. Murooka, and M. Hayashi. 2009. Gibberellin controls the nodulation signaling pathway in *Lotus japonicus*. *Plant Journal* 58: 183–194.

Marco, D. E., J. P. Carbajal, S. Cannas, R. Pérez-Arnedo, A. Hildalgo-Perea, J. Olivares, J. E. Ruiz-Sainz, and J. Sanjuán. 2009. An experimental and modelling exploration of the host-sanction hypothesis in legume–rhizobia mutualism. *Journal of Theoretical Biology* 259: 423–433.

Maruya, J., and K. Saeki. 2010. The *bacA* gene homolog, mlr7400, in *Mesorhizobium loti* MAFF303099 is dispensable for symbiosis with *Lotus japonicus* but partially capable of supporting the symbiotic function of *bacA* in *Sinorhizobium meliloti*. *Plant & Cell Physiology* 51: 1443–1452.

Mathu, S., L. Herrmann, P. Pypers, V. Matiru, R. Mwirichia, and D. Lesueur. 2012. Potential of indigenous bradyrhizobia versus commercial inoculants to improve cowpea (*Vigna unguiculata* L. Walp.) [sic] and green gram (*Vigna radiata* L. Wilczek.) [sic] yields in Kenya. *Soil Science and Plant Nutrition* 58: 750–763.

Maunoury, N., M. Redondo-Nieto, M. Bourcy, W. Van de Velde, B. Alunni, P. Laporte, P. Durand, et al. 2010. Differentiation of symbiotic cells and endosymbionts in *Medicago truncatula* nodulation are coupled to two transcriptome-switches. *PLoS One* 5: e0009519.

Mergaert, P., T. Uchiumi, B. Alunni, G. Evanno, A. Cheron, O. Catrice, A.-E. Mausset, et al. 2006. Eukaryotic control on bacterial cell cycle and differentiation in the *Rhizobium*–legume symbiosis. *Proceedings of the National Academy of Sciences, USA* 103: 5230–5235.

Moawad, M., and E. L. Schmidt. 1987. Occurrence and nature of mixed infections in nodules of field-grown soybeans (*Glycine max*). *Biology and Fertility of Soils* 5: 112–114.

Mueller, U. G., and J. L. Sachs. 2015. Engineering microbiomes to improve plant and animal health. *Trends in Microbiology* 23: 606–617.

Oono, R., C. G. Anderson, and R. F. Denison. 2011. Failure to fix nitrogen by non-reproductive symbiotic rhizobia triggers host sanctions that reduce fitness of their reproductive clonemates. *Proceedings of the Royal Society, B, Biological Sciences* 278: 2698–2703.

Oono, R., R. F. Denison, and E. T. Kiers. 2009. Controlling the reproductive fate of rhizobia: How universal are legume sanctions? *New Phytologist* 183: 967–979.

Paau, A. S., C. B. Bloch, and W. J. Brill. 1980. Developmental fate of *Rhizobium meliloti* bacteroids in alfalfa nodules. *Journal of Bacteriology* 143: 1480–1490.

Pérez Guerra, J. C., G. Coussens, A. De Keyser, R. De Rycke, S. De Bodt, W. Van De Velde, S. Goormachtig, and M. Holsters. 2010. Comparison of developmental and stress-induced nodule senescence in *Medicago truncatula*. *Plant Physiology* 152: 1574–1584.

Porter, S. S., and E. L. Simms. 2014. Selection for cheating across disparate environments in the legume–rhizobium mutualism. *Ecology Letters* 17: 1121–1129.

Prell, J., J. P. White, A. Bourdes, S. Bunnewell, R. J. Bongaerts, and P. S. Poole. 2009. Legumes regulate *Rhizobium* bacteroid development and persistence by the supply of branched-chain amino acids. *Proceedings of the National Academy of Sciences, USA* 106: 12477–12482.

Puppo, A., K. Groten, F. Bastian, R. Carzaniga, M. Soussi, M. M. Lucas, M. R. de Felipe, et al. 2005. Legume nodule senescence: Roles for redox and hormone signalling in the orchestration of the natural aging process. *New Phytologist* 165: 683–701.

Quigley, P. E., P. J. Cunningham, M. Hannah, G. N. Ward, and T. Morgan. 1997. Symbiotic effectiveness of *Rhizobium leguminosarum* bv. *trifolii* collected from pastures in south-western Victoria. *Australian Journal of Experimental Agriculture* 37: 623–630.

Ratcliff, W. C., and R. F. Denison. 2008. Poly-3-hydroxybutyrate (PHB) supports survival and reproduction in starving rhizobia. *FEMS Microbiology Letters* 65: 391–399.

Regus, J. U., K. A. Gano, A. C. Hollowell, and J. L. Sachs. 2014. Efficiency of partner choice and sanctions in *Lotus* is not altered by nitrogen fertilization. *Proceedings of the Royal Society, B, Biological Sciences* 281: 20132587.

Regus, J. U., K. A. Gano, A. C. Hollowell, V. Sofish, and J. L. Sachs. 2015. *Lotus* hosts delimit the mutualism–parasitism continuum of *Bradyrhizobium*. *Journal of Evolutionary Biology* 28: 447–456.

Reid, D. E., B. J. Ferguson, S. Hayashi, Y.-H. Lin, and P. M. Gresshoff. 2011. Molecular mechanisms controlling legume autoregulation of nodulation. *Annals of Botany* 108: 789–795.

Sachs, J. L., M. O. Ehinger, and E. L. Simms. 2010a. Origins of cheating and loss of symbiosis in wild *Bradyrhizobium*. *Journal of Evolutionary Biology* 23: 1075–1089.

Sachs, J. L., S. W. Kembel, A. H. Lau, and E. L. Simms. 2009. In situ phylogenetic structure and diversity of wild *Bradyrhizobium* communities. *Applied and Environmental Microbiology* 75: 4727–4735.

Sachs, J. L., U. G. Mueller, T. P. Wilcox, and J. J. Bull. 2004. The evolution of cooperation. *Quarterly Review of Biology* 79: 135–160.

Sachs, J. L., J. E. Russell, and A. C. Hollowell. 2011a. Evolutionary instability of symbiotic function in *Bradyrhizobium japonicum*. *PLoS One* 6: e26370.

Sachs, J. L., J. E. Russell, Y. E. Lii, K. C. Black, G. Lopez, and A. S. Patil. 2010b. Host control over infection and proliferation of a cheater symbiont. *Journal of Evolutionary Biology* 23: 1919–1927.

Sachs, J. L., R. G. Skophammer, and J. U. Regus. 2011b. Evolutionary transitions in bacterial symbiosis. *Proceedings of the National Academy of Sciences, USA* 108: 10800–10807.

Sato, S., Y. Nakamura, T. Kaneko, E. Asamizu, T. Kato, M. Nakao, S. Sasamoto, et al. 2008. Genome structure of the legume, *Lotus japonicus*. *DNA Research* 15: 227–239.

Schneider, C. A., W. S. Rasband, and K. W. Eliceiri. 2012. NIH Image to ImageJ: 25 years of image analysis. *Nature Methods* 9: 671–675.

Schumpp, O., and W. J. Deakin. 2010. How inefficient rhizobia prolong their existence within nodules. *Trends in Plant Science* 15: 189–195.

Sheehy, J. E., F. R. Minchin, and J. F. Witty. 1983. Biological control of the resistance to oxygen flux in nodules. *Annals of Botany* 52: 565–571.

Shimoda, Y., H. Mitsui, H. Kamimatsuse, K. Minamisawa, E. Nishiyama, Y. Ohtsubo, Y. Nagata, et al. 2008. Construction of signature-tagged mutant library in *Mesorhizobium loti* as a powerful tool for functional genomics. *DNA Research* 15: 297–308.

Simms, E. L., D. L. Taylor, J. Povich, R. P. Shefferson, J. L. Sachs, M. Urbina, and Y. Tausczik. 2006. An empirical test of partner choice mechanisms in a wild legume–rhizobium interaction. *Proceedings of the Royal Society, B, Biological Sciences* 273: 77–81.

Singleton, P. W., and K. R. Stockinger. 1983. Compensation against ineffective nodulation in soybean. *Crop Science* 23: 69–72.

Soltis, D. E., P. S. Soltis, D. R. Morgan, S. M. Swensen, B. C. Mullin, J. M. Dowd, and P. G. Martin. 1995. Chloroplast gene sequence data suggest a single origin of the predisposition for symbiotic nitrogen fixation in angiosperms. *Proceedings of the National Academy of Sciences, USA* 92: 2647–2651.

Somasegaran, P., and J. Hoben. 1994. Handbook for rhizobia. Springer-Verlag, New York, New York, USA.

Tang, J., E. S. P. Bromfield, N. Rodrigue, S. Cloutier, and J. T. Tambong. 2012. Microevolution of symbiotic *Bradyrhizobium* populations associated with soybeans in east North America. *Ecology and Evolution* 2: 2943–2961.

Thapanapongworakul, N., M. Nomura, Y. Shimoda, S. Sato, S. Tabata, and S. Tajima. 2010. NAD^+-malic enzyme affects nitrogenase activity of *Mesorhizobium loti* bacteroids in *Lotus japonicus* nodules. *Plant Biotechnology* 27: 311–316.

Thomas, H. 2013. Senescence, ageing and death of the whole plant. *New Phytologist* 197: 696–711.

Trainer, M. A., and T. C. Charles. 2006. The role of PHB metabolism in the symbiosis of rhizobia with legumes. *Applied Microbiology and Biotechnology* 71: 377–386.

van Berkum, P., P. Elia, Q. Song, and B. D. Eardly. 2012. Development and application of a multilocus sequence analysis method for the identification of genotypes within genus *Bradyrhizobium* and for establishing nodule occupancy of soybean (*Glycine max* L. Merr). *Molecular Plant-Microbe Interactions* 25: 321–330.

Van de Velde, W., J. C. Pérez Guerra, A. De Keyser, R. De Rycke, S. Rombauts, N. Maunoury, P. Mergaert, et al. 2006. Aging in legume symbiosis. A molecular view on nodule senescence in *Medicago truncatula*. *Plant Physiology* 141: 711–720.

Van de Velde, W., G. Zehirov, A. Szatmari, M. Debreczeny, H. Ishihara, Z. Kevei, A. Farkas, et al. 2010. Plant peptides govern terminal differentiation of bacteria in symbiosis. *Science* 327: 1122–1126.

van Doorn, W. G. 2011. Classes of programmed cell death in plants, compared to those in animals. *Journal of Experimental Botany* 62: 4749–4761.

Vance, C. P. 2008. Carbon and nitrogen metabolism in legume nodules. *In* M. J. Dilworth, E. K. James, J. I. Sprent, and W. W. Newton [eds.], Nitrogen-fixing leguminous symbiosis, vol. 7, 293–320. Springer, Dordrecht, Netherlands.

Wang, D., J. Griffitts, C. Starker, E. Fedorova, E. Limpens, S. Ivanov, T. Bisseling, and S. Long. 2010. A nodule-specific protein secretory pathway required for nitrogen-fixing symbiosis. *Science* 327: 1126–1129.

West, S. A., E. T. Kiers, I. Pen, and R. F. Denison. 2002a. Sanctions and mutualism stability: When should less beneficial mutualists be tolerated? *Journal of Evolutionary Biology* 15: 830–837.

West, S. A., E. T. Kiers, E. L. Simms, and R. F. Denison. 2002b. Sanctions and mutualism stability: Why do rhizobia fix nitrogen? *Proceedings of the Royal Society, B, Biological Sciences* 269: 685–694.

Weyl, E. G., M. E. Frederickson, D. W. Yu, and N. E. Pierce. 2010. Economic contract theory tests models of mutualism. *Proceedings of the National Academy of Sciences, USA* 107: 15712–15716.

White, J., J. Prell, E. K. James, and P. Poole. 2007. Nutrient sharing between symbionts. *Plant Physiology* 144: 604–614.